J. Membrane Biol. 58, 139–153 (1981)

The Journal of
Membrane Biology

Mechanism of Cl^- Transport at the Plasma Membrane of *Chara corallina*: II. Transinhibition and the Determination of H^+/Cl^- Binding Order from a Reaction Kinetic Model

Dale Sanders* and Ulf-Peter Hansen

Botany School, Cambridge CB2 3EA, England, and Institut für Angewandte Physik, Neue Universität, 23 Kiel, West Germany

Summary. Internal Cl^- and low internal pH are strong inhibitors of Cl^- influx at the plasma membrane of *Chara*. The present investigation seeks to understand the mechanism by which this is achieved. Since both Cl^- and H^+ are transported by the same system, one possible mechanism is simply through a change in the electrochemical gradients of these ions. However, it is found that transport is more sensitive to the *internal* concentrations of the two ions than to their respective gradients. It is demonstrated that Cl^- influx, which shows Michaelis-Menten kinetics with respect to external concentration, is affected only in its V_{max} by internal Cl^- and pH; the apparent K_m of the transport system for external Cl^- is unchanged. In addition, it is found that there is an apparent interaction between internal Cl^- and pH in their effects on Cl^- influx, both in intact cells and those that have been perfused internally. A kinetic model is proposed which can account quantitatively for all these observations simply through the effects of substrate concentration on the apparent rate constants of a recycling carrier. The model predicts (i) strictly ordered binding of Cl^- and H^+ to the carrier at both internal and external surfaces, with Cl^- first on and first off (ii) movement of charge through the membrane on the loaded, rather than the unloaded, carrier. The present model is expected to account for similar kinetic observations from a variety of other cotransport systems.

Plant cells require a considerable ability to regulate metabolism over a wide range of environmental conditions. This contrasts with the situation in animal cells where the cellular environment is maintained relatively constant by the vascular system, and homeostatic regulation is accomplished far more at a tissue or organ level.

With respect to the control of ion transport in plants, two factors are generally recognized as constituting major set points for regulatory systems: those of turgor pressure and of internal ion concentration (Cram, 1976).

In spite of the importance and widespread occurrence of homeostatic regulation of ion transport in plants, little is known concerning the mechanism of such regulation. Control of ion transport by internal ion concentration has been proposed to occur, for K^+ in several species, through allosteric interaction of internal inhibitor sites (Glass, 1976; Jensen & Petterson, 1978). However, this proposal has been criticised (Sanders, 1980b) on the basis that whilst the ion fluxes observed are those across the plasma membrane, measured changes of internal ion concentration are primarily those in an entirely separate compartment (the vacuole). It is not therefore justifiable in these cases to suggest specific forms of molecular interaction between the transport system and internal ions.

The development of a technique for intracellular perfusion of Characean cells (Williamson, 1975; Tazawa, Kikuyama & Shimmen, 1976) facilitates investigation of the effects of internal ion concentration on ion transport processes at a single membrane: during perfusion the tonoplast is removed and this enables direct contact between the perfusion solution and the inside of the plasma membrane. In the present work, this technique has been applied to the study of the mechanism of control of Cl^- transport at the plasma membrane of *Chara*.

Cl^- influx in *Chara* is mediated by a system transporting H^+ and Cl^- in a probable stoichiometric ratio of 2H/Cl (Sanders, 1978, 1980*c*; Biebyl & Walker, 1980*a*, *b*). It is known that Cl^- influx can be

* *Present address:* Department of Physiology, Yale Medical School, 333 Cedar Street, New Haven, Connecticut 06510.

0022-2631/81/0058-0139 $03.00

controlled by internal Cl^- concentration ($[Cl^-]_i$) and also by internal and external pH (Sanders, 1980*b, c*). One possible mechanism of transport control by pH and $[Cl^-]_i$ could therefore simply be variation of the free energy of the transport reaction. This would be expected were the transport reaction at, or near, thermodynamic equilibrium. Alternatively, the form of control by $[Cl^-]_i$, pH_i and pH_o could be kinetic. In this case a range of possible mechanisms exists, including nonspecific effects of pH on the transport system and the existence of allosteric sites.

In the present paper, we examine the effect of various internal conditions on the kinetics of the transport system, with the aim of constructing a model for the control of Cl^- transport. We have tried to assess to what extent control of transport can be described by the simplest model for the transport process. This consists of binding of substrate externally and internally and transmembrane reactions for the loaded and unloaded carrier. A variety of these models exists, each consisting of a different spatial arrangement of the component reactions. The results of experiments presented here rule out all but one of these models. That which remains, however, is capable of predicting, both qualitatively and quantitatively, all the kinetic observations made on the transport system.

Materials and Methods

Biological material. Cells of the giant alga *Chara corallina* were cultured as described by Sanders (1980*a*). The internodal cells were freed from their neighbors the day before an experiment and bathed overnight in artifical pond water (APW) unless otherwise stated. The composition of APW was (in mM): NaCl, 1; K_2SO_4, 0.2; $CaSO_4$, 1; MES-NaOH, 2; at pH 5.5.

Measurement of Cl^- influx in intact cells was as given by Sanders (1980*a*). Influx was followed in the light for a period of 0.3 ksec: at times longer than this there may be significant generation of secondary effects of applied treatments, particularly as a result of Cl^- starvation which enhances influx (Sanders, 1980*b*). Cl^- starvation effects may be expected to arise during experiments in which influx is measured as a function of $[Cl^-]_o$. However, reference to Figs. 2 and 4 of Sanders (1980*b*) shows that no significant changes in Cl^- transport are apparent in the first 0.3 ksec at the new concentration.

Nomenclature. Internal Cl^- concentration in perfused cells and cytoplasmic Cl^- concentration in intact cells are both referred to as $[Cl^-]_i$. A broad justification for the equivalence of these two parameters is given by Sanders (1980*b*). All experiments on intact cells were conducted over periods short enough to make changes in vacuolar Cl^- concentration insignificant. Similarly, internal pH (perfused cells) and cytoplasmic pH (intact cells) are both designated as pH_i. To avoid confusion with internal concentrations, inhibition constants are designated K_I instead of the more usual K_i.

All transport rates reported in this paper are for unidirectional (tracer) influx.

The intracellular perfusion technique and methods for the measurement of ion fluxes in perfused cells were as given by Sanders (1980*b*). Perfusion removes the vacuolar membrane, thereby giving direct access of the perfusion medium to the inside of the plasma membrane.

Using this system of perfusion, the membrane potential appears to rest at the K^+ equilibrium potential (about -100 mV) and differs from that in intact cells in being insensitive to pH. A detailed consideration of the suitability of perfused cells for transport studies has been presented previously (Sanders, 1980*c*), but it should be added that, so far as Cl^- transport is concerned, evidence is accumulating that no major changes take place after perfusion. Thus, microelectrode measurements of intact cells suggest pH_i is 7.75 (Keifer, 1980) and $[Cl^-]_i$ is 10 mM (Coster, 1966) under standard external conditions. After intracellular perfusion of cells with a medium of exactly this composition, Cl^- influx was measured as $14.7 \pm 3.5(5)$ nmol m^{-2} sec^{-1}. This compares well with Cl^- influx normally measured in intact cells (10 to 20 nmol m^{-2} sec^{-1}) (Hope & Walker, 1975). In addition, evidence has been presented which is consistent with the control of Cl^- influx both in intact and perfused cells by $[Cl^-]_i$ and pH_i (Sanders, 1980*b, c*). Nevertheless, as a further check on the reliability of the perfused cell system, experiments on the kinetics of Cl^- transport in intact cells are also reported in this paper.

In neither intact nor perfused cells is the membrane potential sensitive by more than 10 mV to the range of Cl^- concentrations used in the present experiments.

Line-fitting on double reciprocal plots was performed by the direct linear plot method of Eisenthal and Cornish-Bowden (1974). This nonparametric method provides a more unbiased estimate of the kinetic parameters than would a least squares fit of such plots.

Cytoplasmic pH (pH_i) of intact cells as a function of external pH (pH_o) was estimated from the relation derived experimentally for *Chara* by Smith and Walker (1976):

$$pH_i = 0.22\ pH_o + 6.28.$$

It is assumed that this relation holds for Cl^--starved cells too. This assumption is supported by evidence showing that Cl^- starvation effects on Cl^- influx in intact cells are wholly explained by changes in $[Cl^-]_i$ (Sanders, 1980*b*); thus none of the other parameters controlling Cl^- influx, of which pH_i is one, appears to change.

Membrane potential in intact cells as a function of pH_o was calculated from Fig. 2 of Smith and Walker (1976). A preliminary survey of the cells used in the present work showed a very similar dependence of membrane potential on pH_o.

Modelling of the kinetic data was performed using the reaction kinetic approach of Gradmann, Hansen and Slayman (1981) and Hansen, Gradmann and Slayman[1] (*see* Appendix). Briefly, a system of differential equations is set up to describe each given "state" of the carrier (N_i) in terms of the rate constants and the other states. (A "state" is here defined as any identifiable conformational or chemical form of the carrier.) The system of differential equations then becomes a set of linear algebraic equations for the steady state ($dN_i/dt = 0$). The unidirectional rate of any reaction is calculated as the product of the reactant concentration(s) and the rate constant. Backward and forward charge-carrying transmembrane reactions are calculated as $k_{io} = k^o_{io} \cdot \exp(u/2)$ and $k_{oi} = k^o_{oi} \cdot \exp(-u/2)$, respectively, where k^o is the rate constant at zero voltage and $u = V(zF/RT)$ with the membrane voltage, V, and z, F, R and T with their usual meanings.

[1] Hansen, U.-P., Gradmann, D., Slayman, C.L. Interpretation of current-voltage relationships for "active" ion transport systems: I. Steady-state reaction-kinetic analysis of class-I mechanisms. (*in preparation*)

In the present case short influx periods were used, so the internal concentration of isotopic Cl^- is effectively zero. Under these conditions the equations are well established (Segel, 1975) which describe isotopic influx mediated by a simple carrier model of four states (inside and outside the cell, free and bound to substrate). However, when more than one substrate binds and more carrier states are added, the equations become rapidly more complicated. A detailed treatment of a six-state model is given in the Appendix. In contrast to most previous treatments of cotransport (e.g., Heinz, Geck and Wilbrandt, 1972), the analysis given here is free of the preliminary assumption that transmembrane movement of the carrier is rate-limiting to the overall transport processes. Numerical analysis of this and similar models was performed on a computer.

Results are presented in the form mean ± SEM. Considerable efforts were made to reduce the variability of Cl^- influx in intact cells, where the SEM for a batch of 10 cells was sometimes as high as 25% of the mean. However, none of the methods tried (reducing or increasing the size of the sample, selection of cells of similar age, appearance or size) had any effect. By contrast, Cl^- fluxes in perfused cells were generally repeatable to within 10%.

Results

A. Is Cl^- Influx Controlled by the Free Energy Gradient of the Transported Ions Cl^- and H^+?

The "thermodynamic approach" is based on the assumption that the flux is determined only by the driving forces acting on the loaded carrier.

In the case of the 2H/Cl cotransport system investigated here (Bielby and Walker, 1980*a*,; Sanders, 1980*c*), the driving force consists of three components, which have to be additive according to the "thermodynamic approach": the Cl^- concentration gradient, the H^+ concentration gradient, and the electrical membrane potential. The reaction kinetic approach does not predict net fluxes without a driving force. However, it takes into account that the coefficients relating the driving forces to the fluxes are not constant, but highly dependent on the reactant concentrations involved in the transport process. Via the rate constants, the absolute values of concentrations can become more important than the driving force (if it is not equal to zero).

The following experiments will show that the thermodynamic approach is not capable of describing the behavior of Cl^- influx in *Chara*.

The driving force for chloride ($\Delta\bar{\mu}_{Cl}$) was diminished either by lowering the external Cl^- concentration ($[Cl^-]_o$) or by raising $[Cl^-]_i$. Table 1 gives the results of experiments on similar batches of perfused cells. Over the range tested, the flux is more sensitive to $[Cl^-]_i$ than to $[Cl^-]_o$, indicating that $\Delta\bar{\mu}_{Cl}$ *per se* has less influence on the transport rate than the absolute value of $[Cl^-]_i$.

The driving force for protons ($\Delta\bar{\mu}_H$) was changed by changing inside and outside pH. In Fig. 1, the Cl^- influxes labeled *A* through *F* and *a* through *f* were obtained over the pH_i range 7.00 to 7.75.

Table 1. Effect of $\Delta\bar{\mu}_{Cl}$ on Cl^- influx in perfused cells

$\Delta\bar{\mu}_{Cl}$/kJ mol^{-1}	$[Cl^-]_i$/mM	$[Cl^-]_o$/mM	Influx/% control
+ 9.7	1	1	100
+12.5	3	1	26.2
	1	0.3	83.1
+15.3	10	1	12.5
	1	0.1	57.0

Cells were perfused internally with perfusion medium of the following composition (in mM): EGTA, 50; TES, 5, $MgSO_4$, 13.8; K_2Na_2ATP, 1; KOH, 138.1; K_2SO_4, 7.2; Na_2SO_4, 9; sorbitol, 131; at pH 7.45. $[Cl^-]_i$ was varied by addition of NaCl at the expense of Na_2SO_4. The external solution was $^{36}Cl^-$-APW +250 mM sorbitol, pH 5.5. Variation of $[Cl^-]_o$ was obtained by exchanging NaCl with Na_2SO_4 at constant $[Na^+]$. For the calculation of $\Delta\bar{\mu}_{Cl}$ the membrane potential was taken as −100 mV: it is not sensitive to $[Cl^-]_i$ or $[Cl^-]_o$ (*see* Materials and Methods). The control flux was 18.4 ± 3.8 (11) nmol^{-2} sec^{-1}. Other values are means for two cells.

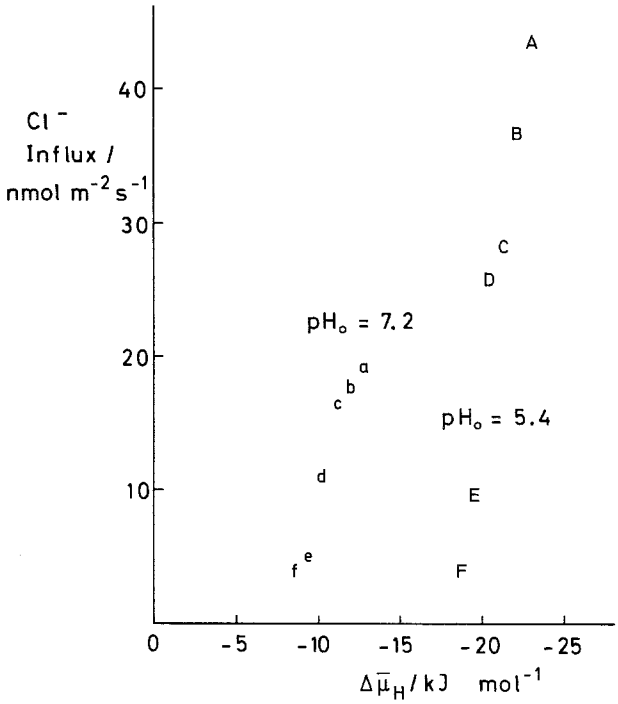

Fig. 1. Effect of $\Delta\bar{\mu}_H$ on Cl^- influx in perfused cells. Cells were perfused internally with a solution of the composition given in Table 1. pH_i was varied by addition of KOH, and K_2SO_4 changed reciprocally to maintain K^+ activity at 43.5 mM. External solution was $^{36}Cl^-$-APW + 250 mM sorbitol. $[Cl^-]_o$ = 1 mM. Capital letters represent data collected with pH_o = 5.4 (i.e., standard APW) over a range of internal pH's 7.00 to 7.75. Lower case letters are similar measurements at pH_o 7.2, with HEPES − NaOH replacing MES as the external pH buffer. For the calculation of $\Delta\bar{\mu}_H$ the membrane potential was taken as −100 mV; it is not sensitive to $[H^+]_i$ or $[H^+]_o$ in perfused cells (*see* Materials and Methods). Each point is for a single cell

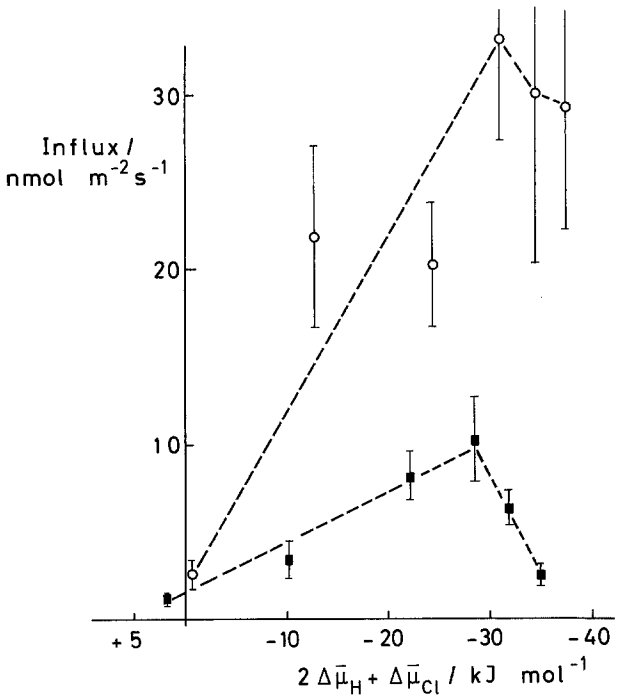

Fig. 2. Response of Cl^- influx in intact cells to ionic driving force (given by $2\Delta\bar{\mu}_H - \Delta\bar{\mu}_{Cl}$). Driving force was varied by changing pH_o or by previous Cl^- starvation to reduce $[Cl^-]_i$. Cells were pretreated overnight in APW with MES substituted by the appropriate buffer. Influx solution was identical to pretreatment solution, but containing $^{36}Cl^-$. Vertical bars are SEM's for batches of 9 to 11 cells. Buffers at final concentration of 2 mM, adjusted with NaOH; pH 4.58 and 5.47, MES; pH 6.40, MOPS; pH 7.28, HEPES; pH 8.23, CHES; pH 9.25, CAPS. Cl^- starvation was accomplished by pretreating cells overnight in APW at the given pH with NaCl substituted by Na_2SO_4 (0.5 mM). The ionic driving force was calculated on the premise that in nonstarved cells $[Cl^-]_i = 10$ mM (■) and in starved cells $[Cl^-]_i = 2.7$ mM (○) (Sanders, 1980*b*). pH_i and membrane potential were calcualted for each pH_o as in Materials and Methods. The dashed lines are simply intended to show the range over which flux may be linear with driving force, though clearly the data do not necessarily justify this. The major point of interest for present purposes, however, is the range of driving force over which the flux responds nonlinearly

In the series labeled by small letters, pH_o was 7.2, and for the capital letters, pH_o was 5.4. If driving force were the only relevant variable, the two series ought to be located on one curve. However, the influence of pH_o, and thus of driving force, is small. This is demonstrated by comparing each capital letter in Fig. 2 with its lower case equivalent: the fluxes differ at most by a factor of only 2.2 (*A*/*a*) in spite of the large change in driving force (approximately 10 kJ mol^{-1}). In comparison, a rise in pH_i corresponding to a change in $\Delta\bar{\mu}_H$ of 4.3 kJ mol^{-1} causes an 11-fold stimulation of flux at pH_o 5.4 and a fivefold change at pH_o 7.2. These experiments show that changes in internal concentrations do not exert their influences on Cl^- influx via the driving force.

A similar large sensitivity to pH_i rather than $\Delta\bar{\mu}_H$ has been found for sugar/H^+ cotransport in *Chlorella* (Komor, Schwab & Tanner, 1979).

The overall driving force for transport was manipulated in intact cells. For a system transporting 2H/Cl, the ionic driving force is given by $2\Delta\bar{\mu}_H + \Delta\bar{\mu}_{Cl}$. Here, $\Delta\bar{\mu}_H$ was manipulated by variation of pH_o: the relevant changes in pH_i and membrane potential have been taken into account in the calculation of $\Delta\bar{\mu}_H$ (*see* Materials and Methods). The results (Fig. 2, lower curve) show that linearity of flux with driving force is maintained up to about -30 kJ mol^{-1}. However, at driving forces greater than this, an inhibition is noted. This has been proposed to result from an inhibitory effect of low pH_i (Sanders, 1980*c*). The $\Delta\bar{\mu}_H$ component of driving force was also varied for cells which had been subjected to prior starvation of Cl^- (Fig. 2, upper curve). The resulting fall of $[Cl^-]_i$ from 10 to 3 mM (Sanders, 1980*b*) is taken into account in the calculation of driving force. Clearly, the small lowering of $\Delta\bar{\mu}_{Cl}$ produced by the fall in $[Cl^-]_i$ results in a greatly increased sensitivity of transport to driving force. Thus even in the range of approximate linearity of flux and force, $\Delta\bar{\mu}_H$ and $\Delta\bar{\mu}_{Cl}$ are not additive in their effects on the flux. If they were, the two curves in Fig. 2 would be superimposable.

Overall, therefore, it may be stated that in intact cells influx shows (i) independence from driving force at high values of the driving force, and (ii) greater effects of Cl^- starvation than would be predicted were starvation acting only on $\Delta\bar{\mu}_{Cl}$—this even over the range of approximate linearity of flux with driving force. An explanation for these observations was therefore sought in kinetic, rather than thermodynamic, terms.

B. Typical Features of the Kinetics of Cl^--Influx

A kinetic treatment, however, has to deal with an anticipated model of the transport system, and thus it depends on the availability of characteristic data which can be used for the construction and the test of the model. Below it is shown that one such typical feature is found in the independence of K_m in contrast to the changes in V_{max} in the presence of internal inhibitors.

Influence of $[Cl^-]_i$ and pH_i on Kinetics of Cl^- Transport in Perfused Cells

Figure 3 shows that the effects of $[Cl^-]_i$ are limited to a lowering of V_{max} for transport: there is no effect on K_m. The K_I for $[Cl^-]_i$ is calculated as 0.55 mM.

With the knowledge that $[Cl^-]_i$ affects only V_{max}, we can also obtain an independent estimate of K_I for

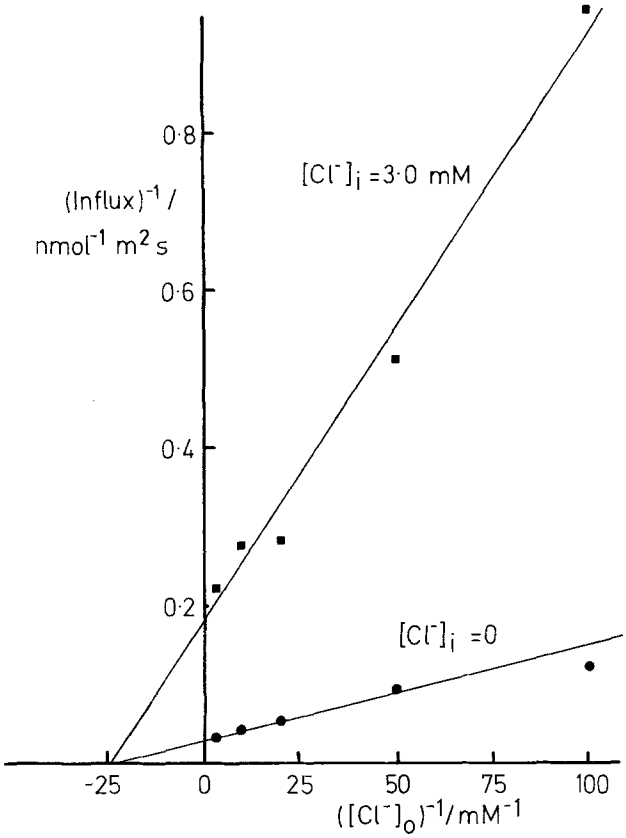

Fig. 3. The effects of $[Cl^-]_i$ on the kinetics of Cl^- influx in perfused cells. Perfusion medium was as described in Table 1, pH 7.45. Variation of $[Cl^-]_o$ was obtained as described in Table 1. Each point is for a single cell. Values of K_m: ($[Cl^-]_i$=0) 41 μM. ($[Cl^-]_i$=3 mM) 40 μM. Values of V_{max}: ($[Cl^-]_i$=0) 33.8 nmol m^{-2} sec^{-1}. ($[Cl^-]_i$=3 mM) 5.4 nmol m^{-2} sec^{-1}. K_I for internal Cl^- is calculated as 550 μM

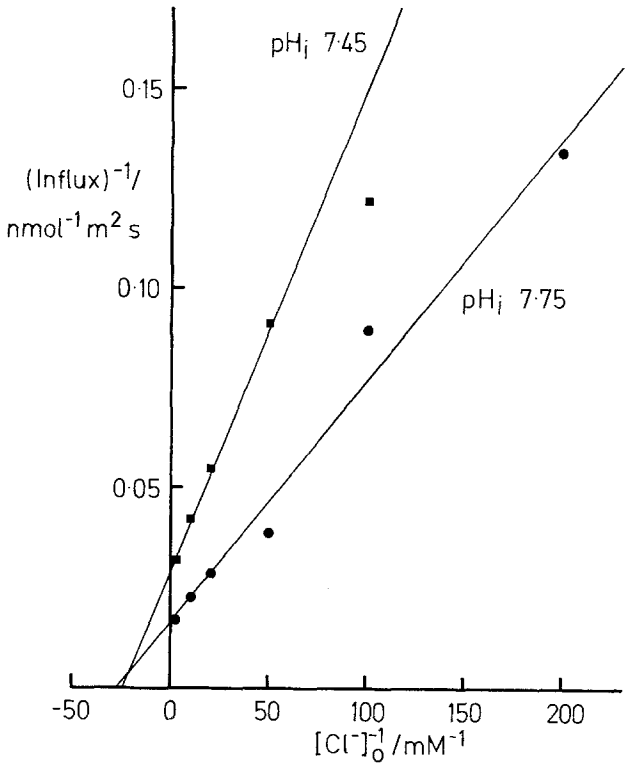

Fig. 4. Effects of pH_i on the kinetics of Cl^- influx in perfused cells. Perfusion medium pH changed as described in Fig. 1. $[Cl^-]_i$=0. $[Cl^-]_o$ changed as described in Table 1. Each point is for a single cell. Values of K_m: pH_i 7.45, 41 μM. pH_i 7.75, 38 μM. Values of V_{max}: pH_i 7.45, 33.8 nmol^{-2} sec^{-1}. pH_i 7.75, 64.5 nmol^{-2} sec^{-1}

Cl_i^- from the data of Sanders (1980*b*). In that case $[Cl^-]_i$ was raised at constant, high, $[Cl^-]_o$ (1 mM $=25K_m$). From the resulting Dixon plot, a K_I of 0.52 mM is estimated – in good agreement with the present estimate which was obtained under similar conditions of pH_i and pH_o by varying $[Cl^-]_o$ at constant $[Cl^-]_i$.

The effects of pH_i are kinetically similar to those of Cl_i^- (Fig. 4). Raising pH_i by 0.3 unit to 7.75 results in a doubling of V_{max} with no significant change in K_m.

In addition to their separate effects on Cl^- influx, there is also an apparent interaction between pH_i and $[Cl^-]_i$. Figure 5 shows that the *proportional* influence of $[Cl^-]_i$ is reduced as pH_i is raised. At pH 7.15, $[Cl^-]_i$ inhibits flux to 30% of control, whereas at pH 7.75 flux is over 80% control in the presence of the same concentration of Cl^- (1 mM).

At high pH_i (Fig. 6) the kinetic effects of $[Cl^-]_i$ are again limited to a lowering of V_{max} (*cf.* Fig. 3). As implied by the data of Fig. 5, the K_I of transport for $[Cl^-]_i$ is now higher than at pH_i 7.45, by a factor of 3.5.

Kinetics of Halide Influx in Intact Cells

a) Effects of $[Cl^-]_i$ are limited to V_{max}: Although the relevant direct measurements have not yet been made, there is strong evidence that during Cl^- starvation of intact cells $[Cl^-]_i$ falls (Sanders, 1980*b*). Therefore, it should be possible to study the effects of $[Cl^-]_i$ on the kinetics of Cl^- transport in intact cells by comparing Cl^--starved and nonstarved cells. In order to do this, influx periods must be kept as short as possible at each external Cl^- concentration, otherwise when transport is reduced at low $[Cl^-]_o$, the ensuing fall of $[Cl^-]_i$ will tend to restore the flux, as discussed in Materials and Methods. However, use of short influx periods can lead to large counting errors when working at low concentrations of $^{36}Cl^-$ (which is only available at low specific activity). Experiments were therefore conducted with $^{82}Br^-$ which has previously been used as an analogue for Cl^- (MacRobbie, 1971).

Over the external concentration range 1–100 μM, Br^- influx can be described by Michaelis-Menten

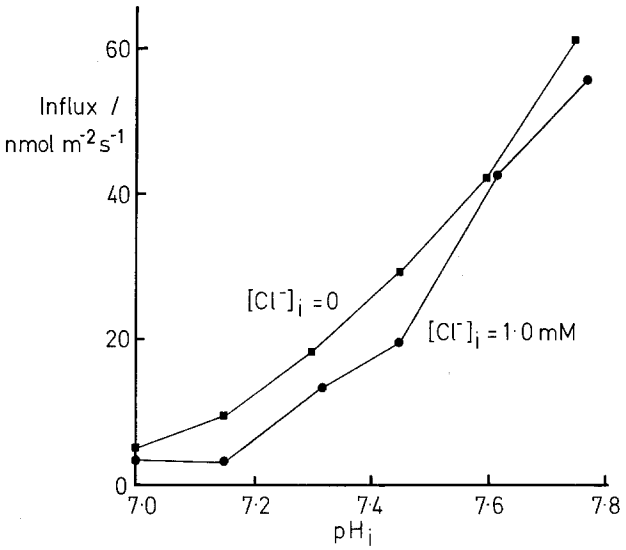

Fig. 5. Effects of internal Cl^- on pH_i response of influx. Variations of $[Cl^-]_i$ and pH_i obtained as in Table 1 and Fig. 1, respectively. External solution was $^{36}Cl^-$-APW + 250 mM sorbitol. Each point is for a single cell

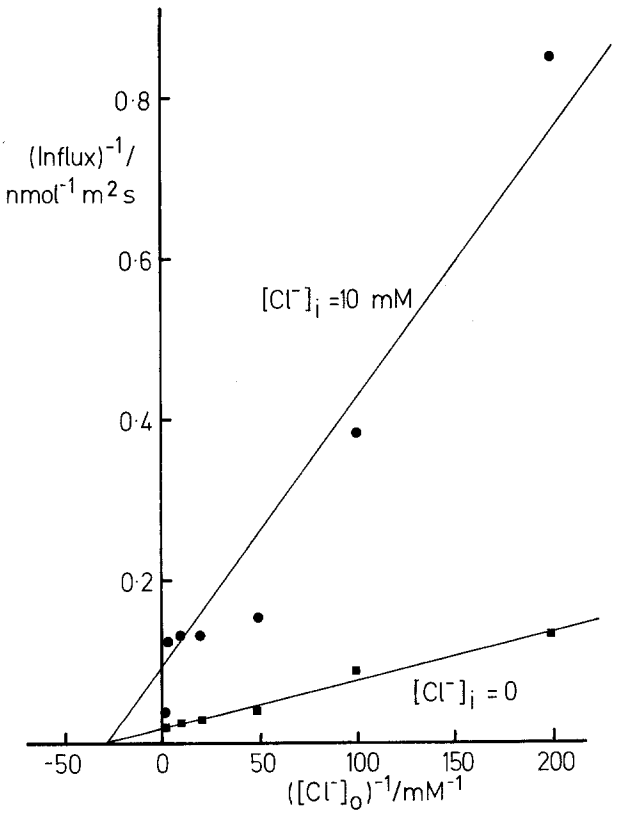

Fig. 6. Effects of internal Cl^- on the kinetics of Cl^- influx at high pH_i (pH 7.75). Methods were as in Fig. 3. Each point is for a single cell K_m ($[Cl^-]_i = 0$) 38 μM. K_m ($[Cl^-]_i = 10$ mM) 35 μM. V_{max} ($[Cl^-]_i = 0$) 64.5 nmol m^{-2} sec^{-1}. V_{max} ($[Cl^-]_i = 10$ mM) 10.6 nmol m^{-2} sec^{-1}. K_I of the transport system for internal Cl^- is 1.94 mM

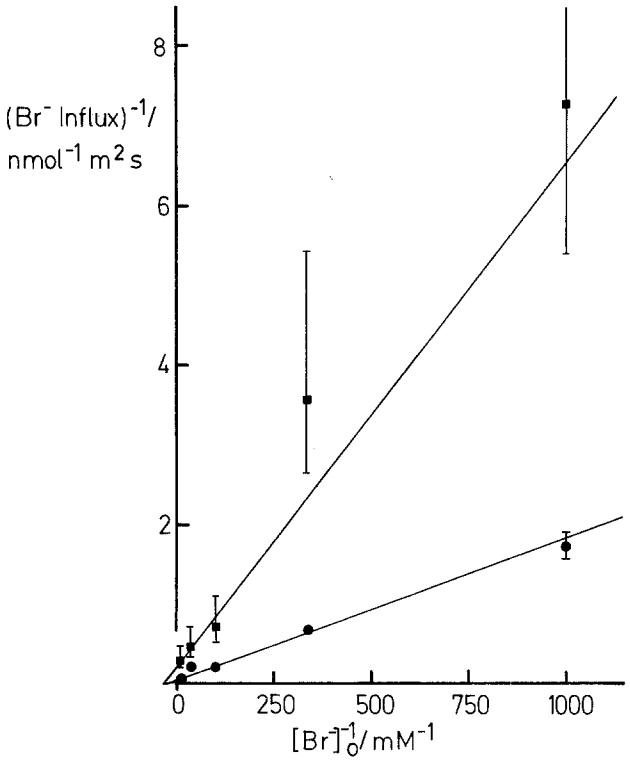

Fig. 7. Kinetics of Br^- influx in intact cells. Batches of 10 cells were pretreated overnight in APW (■) or Cl^--free APW (●). After 10-sec wash in Cl^--free APW (to prevent contamination of influx solution with Cl^-) influx was measured in $^{82}Br^-$ APW. Composition of Br^--APW (in mM): 0.2, K_2SO_4; 2, Na^+ as NaBr or Na_2SO_4; 1, $CaSO_4$; 2, MES-NaOH; pH 5.5. K_m (starved cells) 36 μM. K_m (nonstarved cells) 27 μM. V_{max} (starved cells) 20.9 nmol m^{-2} sec^{-1}. V_{max} (nonstarved cells) 4.3 nmol m^{-2} sec^{-1}

kinetics, both for starved and nonstarved cells (Fig. 7). As is found for perfused cells, the effect of high $[Cl^-]_i$ is limited to lowering V_{max} of influx: K_m is unaffected. Thus, qualitatively, these data support the conclusions arrived at for perfused cells.

b) Further evidence for pH_i-dependence of K_I of transport for $[Cl^-]_i$: Figure 8 shows that, compared with nonstarved cells, the inhibitory effect of low pH_o on Cl^- influx in Cl^--starved cells is much reduced. This effect was noted consistently, and is clearly marked at pH_o 4.5. It was proposed previously (Sanders, 1980*c*) that inhibition of influx at low pH_o is indirect: the inhibition results from the lowering of pH_i at low pH_o. If this is the case, then the result in Fig. 8 is fully in accord with the foregoing experiments showing that low pH_i tends to decrease the K_I of transport for $[Cl^-]_i$ in perfused cells: when $[Cl^-]_i$ is low, as it appears to be in Cl^--starved cells, the effects of pH_i on the flux will be relatively smaller. In other words, low pH_i acts not only directly to inhibit transport, but also inhibits by increasing the sensitivity of transport to $[Cl^-]_i$.

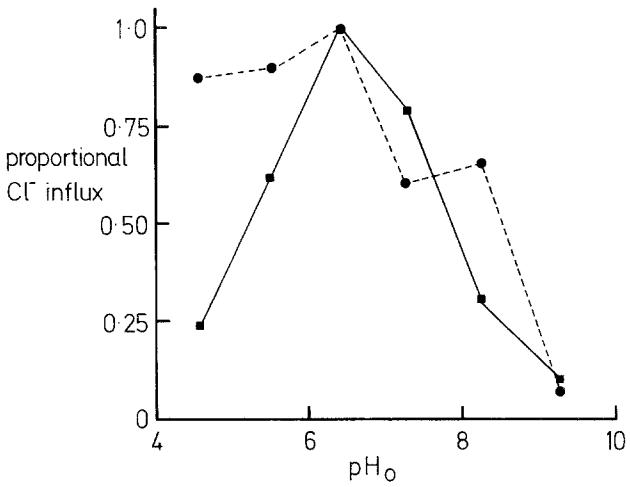

Fig. 8. Cl^- influx in intact cells as a function of external pH. Data of Fig. 2 were replotted. Control fluxes (at pH_o 6.4): Cl^--starved cells (●) 33.2 ± 6.5 nmol m^{-2} sec^{-1}. Nonstarved cells (■) 10.3 ± 2.4 nmol m^{-2} sec^{-1}. Standard errors (not shown for reasons of clarity) were about 20% of the mean

Discussion

A. Is the Cl^- Transport System at Reversible Equilibrium?

The description of ion transport in giant algae has previously been considered primarily in terms of variation of the energy supply (driving force) (*see*, e.g., Raven, 1976). The experiments described above make it clear that considering only the driving force *per se* does not result in an adequate prediction of the measured rates of transport, at least in the case of Cl^- influx. The conclusion that Cl^- transport in *Chara* is primarily under kinetic control was also reached by Raven and Smith (1978).

Nevertheless, it would not be correct to state that Cl^- influx is insensitive to driving force. Figure 2 shows that such an influence is indeed found in the neighborhood of thermodynamic equilibrium (driving force = 0). In Table 1 and Fig. 1 there is also a small effect of the driving force. In addition, Bielby and Walker (1980*b*) have shown that, if membrane potential is changed from -100 to -200 mV, the Cl^- current is stimulated by a factor of 1.8.

However, the majority of the experiments presented above indicate more complicated relationships than those covered by the concept of driving forces. Below, we investigate the nature of these relationships more thoroughly by developing the reaction kinetic approach of Gradmann et al. (1981). This model can be used to account for the effects of reactants on influx without resorting to the labels of "kinetic" *vs.* "thermodynamic" control. The reaction kinetic approach takes account of the whole spectrum of situations between these extremes where both kinetic *and* thermodynamic considerations must be made. The model therefore predicts an influence of driving force on ion flux, but one which progressively diminishes as deviation from equilibrium is attained.

B. Generation of a Model

Application of the reaction kinetic approach to Cl^- transport in Chara: In the following treatment, all pH effects on transport are considered in terms of H^+ as a cosubstrate for the Cl^- transport system. Although nonspecific pH effects cannot be ruled out, it will be shown that the influence of H^+ on kinetics of Cl^- transport can be incorporated into a simple transport model. Therefore, it is unnecessary to postulate that pH has additional effects.

Any working kinetic model must explain the five primary observations reported in this paper:

1) Cl^- influx displays Michaelis-Menten kinetics with respect to external Cl^-.

2) $[Cl^-]_i$ acts to lower V_{max} of influx with no effect on K_m.

3) Low pH_i similarly behaves as a noncompetitive inhibitor.

4) At high pH_i, the K_I for $[Cl^-]_i$ is raised.

5) Raising pH_i by 0.75 unit produces a 10- to 20-fold stimulation of Cl^- influx.

To this list can be added another property of Cl^- influx in perfused cells reported previously (Sanders, 1980*b*):

6) V_{max} for Cl^- influx is reciprocally related to $[Cl^-]_i$.

The minimum model for cotransport of Cl^- with $2H^+$ consists of eight reactions: three surface reactions on either side of the membrane as each substrate binds and dissociates, and two trans-membrane reactions of the fully loaded carrier and the unloaded carrier. In Fig. 9*A*, the $2H^+$ binding steps have been merged into one on the assumption that each binding site has the same pK and acts independently: the apparent rate constants will therefore vary as the square of the H^+ concentration.

The rate equations describing the influx of chloride mediated by this model are given in the Appendix. These equations will be used to check whether the model explains the observations listed above and to disprove alternative arrangements of the binding reactions.

1) Eq. (A28) shows that the model predicts Michaelis-Menten kinetics.

2 & 3) The independence of K_m from $[Cl^-]_i$ and from pH_i is discussed with reference to Eq. (A33). This is the simplified form of the full expression for K_m (Eq. (A30)). The simplification arises from the fact

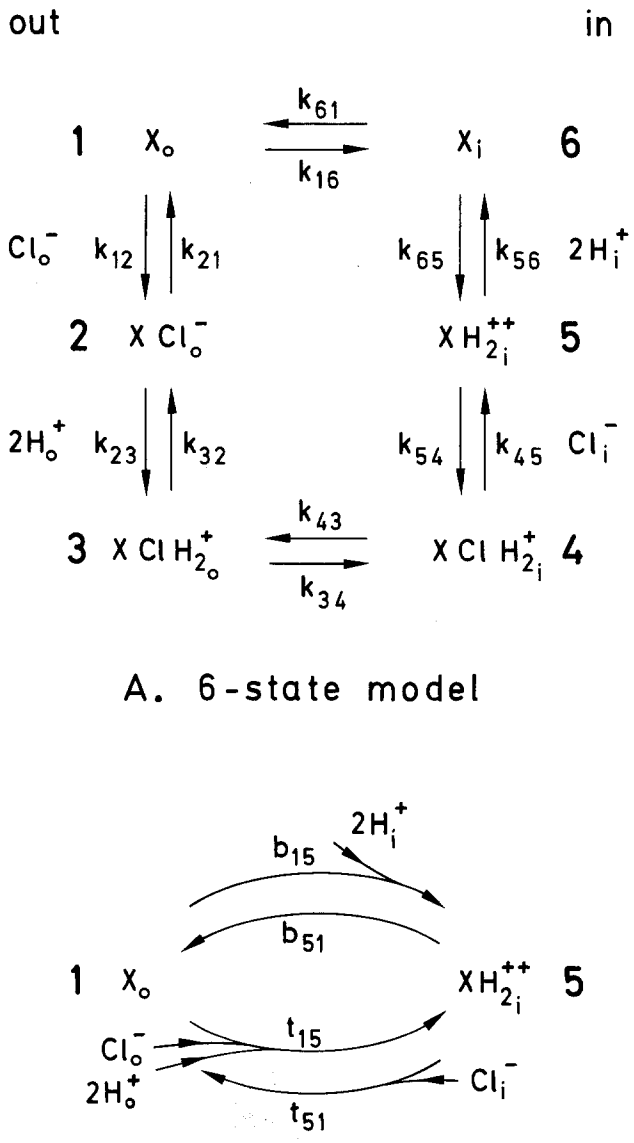

Fig. 9. Model for the sequence of carrier reactions for Cl^- influx according to the surface asymmetry model. Under normal conditions, $[H^+]_o$ will be high compared with the pK of the transport site, and it is postulated that this reaction provides the primary driving force. In intact cells, the membrane potential of -170 mV will contribute considerably to the driving force, also. In perfused cells where the membrane potential is about -100 mV, it will assume lesser importance: it is primarily the displacement of the external protonation reaction towards the quaternary complex which accounts for the kinetic effects of internal inhibitors. (*A*): The full working model, as used in the algebraic and numerical analyses. Justification for the binding sequence is given in text. (*B*): Simplification of *A*: *see* Appendix for details

that influx via the 2H/Cl transport system is energized partly by the membrane potential and partly by the chemical gradient for H^+. Membrane potential of -100 mV induces an asymmetry in the rate constants k_{34}/k_{43}, as described in Materials and Methods. The chemical gradient for H^+ could be proposed to act either on the internal or the external binding reactions for H^+, or both. We assume the energization from the chemical H^+ gradient is reflected exclusively at the *external* binding reactions (Eq. (A31*a*)) for the reasons that (i) transport in perfused cells is saturated with H_o^+ at pH_o 5.5 (Sanders, 1980*c*). These were the conditions used in all the experiments in the present work. (ii) The apparent pK of the internal H^+ binding sites is 7.85 (Sanders, 1980*c*), so in the present experiments these reactions would be close to equilibrium.

There seem to be two different situations which make the dependency of K_m on Cl_i and pH_i vanish:

a. The terms comprising no A and no B (i.e., those independent of pH_i and $[Cl^-]_i$) have to be small. This cannot be verified, since A^* is 1 at pH 7.75 (*see* Eq. (A38*b*)) and k_{61}/k_{61} is equal to 1, too.

b. The condition given by Eq. (A35) has to hold. A complete independence of K_m on Cl_i (B^*) and on pH_i(A^*) is obtained if $k_{16}=k_{45}$ and $k_{56}\gg k_{16}$ B^*.

These two conditions are not unlikely. It is reasonable that k_{56}, which is due to a deprotonization, is a very rapid reaction more rapid than the crossing of the membrane by the unloaded carrier.

However, even deviations from the above conditions will lead only to minor changes in K_m with pH_i or Cl_i, as shown by the numerical analysis below.

The data in Figs. 3, 4 and 6 can be used to get some information about the rate-constants in the model of Fig. 9. Figure 4 gives $V_{max}=64.5$ nmol m^{-2} sec^{-1} at $pH_i=7.75$ ($h^2=1$ by definition of q_h in Eq. A38*b*) and $V_{max}=33.8$ nmol m^{-2} sec^{-1} at $pH_i=7.45$ ($h^2=4$). As $[Cl]_i=0$ in this experiment, the insertion of these data into Eq. (A40) results in

$$33.8(4+\text{const})=64.5(1+\text{const}). \tag{1}$$

From this,

$$\text{const}=2.3. \tag{2}$$

Making use of the condition for constant K_m (Eq. (A35)) we obtain the following relation from Eq. (A41)

$$q_h=\frac{1}{2.3}\left(1+\frac{k_{61}}{k_{16}}\right). \tag{3}$$

The value of q_h is interesting as it is the ratio of binding and dissociation of H_i at $pH_i=7.75$. It is difficult to get more information about q_h because it occurs as a factor in Eq. (A40), which is lost when quotients are determined as in Eq. (1). q_b, containing the ratio of binding and dissociation of Cl_i at $[Cl]_i=1$ mM, can be obtained from the data in Fig. 3.

There, insertion into Eq. (A40) leads to

$$5.4(4(1+3q_b)+\text{const})=33.8(4+\text{const}) \quad (4)$$

resulting in

$$q_b=\frac{k_{12}k^o_{54}}{k_{34}k_{45}}=2.8\ \text{mM}^{-1}. \quad (5)$$

The data of Fig. 6 give

$$q_b=1.8\ \text{mM}^{-1}. \quad (6)$$

However, as with the data for H^+, Eqs. (5) and (6) do not give the value of binding constant of Cl^- (k^o_{54}/k_{45}) explicitly: q_b comprises the rate constants k_{12} and k_{34} in addition to k^o_{54} and k_{45}.

The values for q_b obtained from Fig. 3 and from Fig. 6 differ by a factor of 1.6. However, given the variety of conditions of pH_i and $[Cl^-]_i$ in which the experiments were performed, the agreement is reasonable.

4) The K_I for $[Cl]_i$ is shown to be pH-dependent by Eq. (A42) in the Appendix. According to the calculations above

$$\begin{aligned} K_I&=0.68\ \text{mM} \quad \text{for} \quad pH_i=7.45\\ K_I&=1.43\ \text{mM} \quad \text{for} \quad pH_i=7.75 \end{aligned} \quad (7)$$

using an average value of $q_b=2.3\ \text{mM}^{-1}$.

Note from this that neither K_I nor K_m is necessarily indicative of the dissociation constant (K_d) for Cl^- binding. K_I can be significantly higher than K_m even if K_d is the same on both sides of the membrane. $K_I > K_m$ is observed experimentally in this system, and for others showing transinhibition (Pall, 1971; Cuppoletti & Segel, 1974).

5) The 10- to 20-fold stimulation of Cl^- influx caused by raising pH_i by 0.75 unit (factor of 31.6 in h^2) can be verified by calculating the relative changes of V_{max} for $pH_i=7.75$ ($h^2=1$) to $pH_i=7.00$ ($h^2=31.6$) by means of Eq. (A37). This results in

$$\text{stim}_o=\frac{31.6+\text{const}}{1+\text{const}}=10.3\text{-fold} \quad \text{for} \quad [Cl_i]=0 \quad (8)$$

$$\text{stim}_1=\frac{31.6(1+q_b)+\text{const}}{1(1+q_b)+\text{const}}=19.0\text{-fold}$$

$$\text{for} \quad [Cl_i]=1\ \text{mM} \quad (9)$$

with $q_b=2.3\ \text{mM}^{-1}$ and const = 2.3.

These values are in excellent agreement with the experimentally-determined one of 12.4-fold ($[Cl^-]_i=0$) and 17.1-fold ($[Cl^-]_i=1$ mM) from Fig. 5. Note that the data of Fig. 5 were obtained completely independently of those used for the estimates in Eqs. (8) and (9).

Table 2. Effect of $[H^+]_i$ and $[Cl^-]_i$ on kinetic parameters of model of Fig. 9*A*

$[Cl^-]_i$	$[H^+]_i$	Representative pH	V_{max}	K_m	K_I for Cl^-_i
0	1.58	7.75	2.11	0.75	
	6.31	7.45	1.06	0.88	
	50.12	7.00	0.19	0.98	
1	1.58	7.75	1.36	0.71	2.22
	6.31	7.45	0.59	0.81	1.29
	50.12	7.00	0.09	0.98	1.02
10	1.58	7.75	0.32	0.63	2.22
	6.31	7.45	0.12	0.86	1.30
	50.12	7.00	0.02	0.98	1.04

Modelling was performed as described in Materials and Methods. Values are all in arbitrary units. All rate constants in Fig. 9*A* were set to 1. $[H^+]_o$ was set to 10^4, i.e., $[H^+]_o$ was 2 pH units above pK of H^+ transport site. Membrane potential was set at -100 mV to act on the trans-membrane reaction of the loaded (positively charged) carrier, and the forward and backward rates of this reaction were adjusted accordingly. To obtain V_{max} and K_m, $[Cl^-]_o$ was varied from 0.1 to 1000, and linear double reciprocal plots for the flux resulted. Variations in $[H^+]_i$ were chosen to represent an apparent pK of the H^+ dissociation sites inside of 7.85 (Sanders, 1980*c*). Thus, at this pH, $[H^+]_i$ was set at 1. Changes in $[H^+]_i$ from this pH are represented as the square of the concentration change, as it is postulated that $2H^+$ transport sites are involved.

6) The reciprocal dependence of V_{max} on $[Cl^-]_i$ is predicted by Eq. (A40).

Thus, it is shown that the model in Fig. 9*A* is capable of explaining all the findings of the reported experiments even in a quantitative manner. As an additional illustration (Table 2), Cl^- influx is calculated from a nonsimplified version of the model in Fig. 9*A* by means of a computer for the set of parameters described in the legend. In modelling, we have assumed that with no net driving force across the system, all rate constants = 1. Although this is, of course, unjustified for the real transport system, it has the virtue that it is capable of accurately regenerating the observed findings without more specific assumptions that certain reactions are intrinsically rate-limiting. Ion concentrations and the membrane potential have then been introduced separately, and the appropriate reaction rates changed accordingly. Thus, with $k_{23}/k_{32}=10^4$ (-22 kJ mol^{-1}) at pH_o 5.4, and $k_{34}/k_{43}=54$ (-9.7 kJ mol^{-1}) for a membrane potential of -100 mV, the primary site of energization has been assigned to the binding of H^+ externally.

Reference to Table 2 shows clearly that the five primary kinetic effects reported here can be duplicated by this very simple minimum model. The sixth property is also demonstrated – K_I is independent of $[Cl^-]_i$. The numerical example verifies all the theoretical considerations outlined above.

Table 3. Numerical predictions of the alternative models to that of Fig. 9*A*.

		Deviation of Model from Fig. 9*A*					
		(a) Cl_i dissociates 2nd; H_i dissociates 1st		(b) Cl_o binds 2nd; H_o binds 1st		(c) Charge transfer step is unloaded carrier	
Cl_i	H_i	V_{max}	K_m	V_{max}	K_m	V_{max}	K_m
0	1.58	2.10	0.42	2.12	0.25	2.30	0.24
	6.31	1.04	0.21	1.06	0.12	2.00	0.23
	50.12	0.19	0.04	0.19	0.02	0.92	0.18
1	1.58	1.36	0.63	1.41	0.16	1.48	0.16
10	1.58	0.32	0.91	0.45	0.05	0.35	0.06

Modelling was carried out as for Table 2, with the changes in binding order noted for each case.

Consideration of the topographically alternative models

(i) The sequence of the binding steps at the inside is crucial for the independence of K_m from Cl_i and pH_i. The reason for this is as follows:

We do not need a new model to discuss a changed order of Cl_i release and H_i release at the inside. We can merge the reactions between 2 and 4 into k_{23} and k_{32}. Then k_{43} can be used for the incorporation of the pH_i sensitivity by assigning the H^+ binding to it. k_{54} keeps its role (Cl_i^--binding), and k_{65} becomes constant. In this model, k_{43} occurs in z_1, z_5 and v_{51} (*see* Eqs. (A15), (A16) and (A5*b*)). Because of the asymmetry caused by the energization, v_{51} can be neglected. z_5 becomes zero for $[Cl]_i = 0$. This is exactly the condition prevailing in Fig. 4, where the influence of pH_i (k_{43} now) is studied in the absence of Cl^-. Thus z_1 is the only remaining pH_i-sensitive term. z_1 occurs only in the denominator of Eq. (A30), which is the same for V_{max} and for K_m. On double reciprocal plots, a decrease in pH_i would therefore essentially increase the absolute values of the intercepts, but leave the slope unchanged (uncompetitive inhibition): clearly this is not observed (Fig. 4). The numerical modelling in Table 3*a* confirms this expectation. In the absence of Cl_i, increasing $[H^+]_i$ under conditions where H_i dissociates first, results in proportionally the same decrease in K_m and V_{max}. The alternative order of Cl_i and H_i from that in Fig. 9*A* cannot, consequently, account for the experimental finding of constant K_m with pH_i-sensitive influx at $Cl_i^- = 0$. Thus, the alternative sequence is ruled out, and the order of Cl_i and H_i in Fig. 9*A* demonstrated to be crucial.

(ii) Analogous arguments show that the sequence of binding of Cl_o^- and H_o^+ is also an essential feature of this model. Again, we can adjust the model of Fig. 9*A* to discuss this. In Appendix II it is shown that the influence of H_o for the case of inverse external binding order (H^+ first, then Cl^-) can be discussed for the condition $k_{61} \gg k_{16}$, which holds at saturating H_o concentrations. In addition, v_{51}^o will be small because of the asymmetry introduced by the membrane potential. Under these conditions, reference to Eq. (A30) (expression for K_m) shows that the dominant term in the numerator is $DENk_{56}k_{61}$ which is both Cl_i- and H_i-independent. On the other hand, in the denominator there exist terms for both Cl_i and H_i which are significant, as they contain no v_{51}^o and are independent of the condition $k_{61} \gg k_{16}$. The common denominator for V_{max} and K_m therefore again leads us to expect equivalent decreases of V_{max} and K_m, this time for both Cl_i^- and H_i^+. The numerical results from the nonsimplified model in Table 3*b* demonstrate this clearly. Thus it is concluded that the correct binding order externally must be Cl^- first, then H^+.

(iii) We consider here the reaction step involved in charge transfer. An alternative possibility to that of Fig. 9*A* is that the unloaded carrier transports negative charge out of the cell during Cl^- influx, with the loaded carrier the neutral species. Under these conditions k_{61} becomes large, k_{16} small and a small value for v_{51}^o is achieved by proton binding at k_{23}. Thus the same arguments as for the case of changed external binding order ((ii) above) hold and K_m and V_{max} should fall in parallel as Cl_i or H_i are raised (*see* Table 3*c*). That this behavior was not observed experimentally leads to the conclusion that charge transfer occurs with the entry of Cl^- (k_{34}).

C. Applicability of the "Surface Asymmetry" Model to Other Transport Systems

One of the essential features of the present model for trans-inhibition is that the saturated (asymmetric) H_o^+-binding step is adjacent to the transmembrane

loaded carrier reaction in order to give rise to the observed kinetic characteristics. Because of this, we term the model the "surface asymmetry" model. This distinguishes it from the more common model for transinhibition, first proposed by Pall (1971), in which an asymmetry (or essential irreversibility) of the transmembrane reaction of the loaded carrier is supposed to account for similar kinetic characteristics. For the *Chara* Cl^- system, there is also transmembrane asymmetry due to the action of the membrane potential in the model proposed here. However, the same kinetic features would occur even in the absence of a membrane potential, as long as H_o^+ binding is saturating.

Many other transport systems share similar kinetic properties to those described here for Cl^- transport; increase of the internal concentration of transport system substrate affects only V_{max} and not K_m. These systems are mainly for amino acid transport in bacteria and fungi (Ring & Heinz, 1966; Crabeel & Grenson, 1970; Pall, 1971; Kotyk & Rihova, 1972; Morrison & Lichtstein, 1976) and also possibly for sucrose transport into the phloem of higher plants (Giaquinta, 1980). In addition, kinetically less well characterized transinhibition has been demonstrated for Cl^- (Russell, 1976) and amino acids (Belkhode & Scholefield, 1969) in animal cells.

There is now good evidence that all of these compounds are cotransported: with H^+ for amino acid transport in microorganisms (Eddy, 1978); with H^+ for sucrose in phloem (Hutchings, 1978); with Na^+ for Cl^- in squid axon (Russell, 1979); and with Na^+ for amino acids in many animal cells (Crane, 1977). Thus it seems likely that the surface asymmetry model proposed here could also apply to the above systems; it is not necessary to propose specifically that the transinhibitional characteristics reside with an asymmetric *transmembrane* reaction.

The most thorough study of transinhibition has been made by Cuppoletti and Segel (1974) for SO_4^{2-} transport in *Penicillium*. Their kinetic approach, which is similar to that taken here, also points out that the noncompetitive nature of the transinhibitor is only achieved under special conditions. Their work revealed that, externally, binding of both H^+ and Ca^{++}, whose entries may power that of SO_4^{2-}, occurs before that of SO_4^{2-} (Cuppoletti & Segel, 1975). Not surprisingly, the kinetic characteristics of transinhibition by SO_{4i}^{2-} are very different from those reported here: internal SO_4^{2-} behaves as a mixed inhibitor (Cuppoletti & Segel, 1974). Thus, noncompetitive kinetics are clearly not a precondition for transinhibition. However, the surface asymmetry proposal explains why noncompetitive kinetics are so frequently obtained – they result both from the high pK of the H^+ transport site and from the specific order of binding and dissociation of substrate and H^+ with carrier.

"First on-first off" binding characteristics have also recently been proposed for Na^+-glucose cotransport in brush border vesicles (Hopfer & Groseclose, 1980). However, the equilibrium exchange conditions under which those experiments were performed did not enable identification of the transport system substrate which binds first.

Evolutionary considerations. Homeostatic functioning of a transport system requires a steep dependence of transport rate on substrate level – usually steeper than can be provided by the influence of driving force. This deviation from thermodynamic behavior can originate from two different mechanisms: from the intrinsic kinetics of the transport system or from adjustment of transport rate by means of a sophisticated feed-back system. In the case of H^+ transport in another Characean, *Nitella*, oscillatory behavior indicates the involvement of a feed-back system (Hansen, 1978; 1980). However, in the case of ions whose concentration is less crucial than that of H^+ for the proper functioning of enzymes, intrinsic kinetics alone may result in adequate control of transport rate. The investigations presented here show that this appears to be the case for Cl^- transport.

This model for transinhibition is conceptually simple and requires no complex evolutionary strategy. The requirements are that the carrier site for H^+ has a pK slightly above cytoplasmic pH. Then, under acid conditions externally, for a system cotransporting $2H^+$ per Cl^- the following characteristics result:

1) Cytoplasmic Cl^- concentration is maintained at a relatively constant level. The transport system shows Michaelis-Menten kinetics for $[Cl^-]_o$ when all other conditions are constant. Operationally, however, the system will shut down when high $[Cl^-]_o$ leads to high transport rate and thus an elevated internal Cl^- concentration.

2) Transport is extremely sensitive to pH_i. Thus, under conditions where pH_i is low, the leak conductance for H^+ is automatically shut down and further acidification prevented.

Both these functions can be considered homeostatic, yet there is no specific property of the transport system which has been evolved solely to this end. The system is auto-regulatory without the need for allosteric sites or a negative feedback system.

However, the system is not capable of regulating $[Cl^-]_i$ around a constant set point which shows *complete* independence from $[Cl^-]_o$. This simple homeostatic mechanism may therefore be characteristic of systems which transport nonessential (but

useful) metabolites into the cell. For substances with a more central metabolic role (for example H^+) it appears that more complex feedback systems are necessary (Hansen, 1978; 1980).

D.S. is grateful to Dr. E.A.C. MacRobbie for supervision of parts of this work, which formed a portion of a doctoral thesis at Cambridge University, and to the Science Research Council (Great Britain) for support during this period. Some of the theoretical parts of this work were carried out in the lab of Dr. C.L. Slayman, to whom we are indebted for helpful discussions. Thanks are also due to Dr. D. Gradmann, for convincing us that kinetic modelling can usefully be applied to biological systems, and to Dr. N.A. Walker for communicating some of his results prior to publication.

Appendix I

The Calculation of the Influx of Labeled Cl^-

The flux of tracer is calculated from the reaction kinetic scheme shown in Fig. 9. Since every conversion of X_o (state 1) to XH_2^{++} (state 5) via the lower pathway results in the translocation of one Cl^- ion from the outside to the inside, the gross reaction t_{15} is a measure of the influx of labeled chloride, ϕ_{in},

$$\phi_{in}=t_{15}[X]_o. \tag{A1}$$

The calculation is done in terms of a pseudo-2-state model shown in Fig. 9*B*. According to the formalisms described by Gradmann et al. (1981) and Hansen et al.[2]

$$\phi_{in}=N_o\frac{\left(\frac{t_{15}b_{51}}{r_1r_5}\right)}{\left(\frac{t_{15}}{r_1}+\frac{t_{51}}{r_5}+\frac{b_{15}}{r_1}+\frac{b_{51}}{r_5}\right)} \tag{A2}$$

with N_o = sum of all carrier states, and

$$b_{15}=\frac{k_{16}k_{65}}{k_{65}+k_{61}} \qquad b_{51}=\frac{k_{56}k_{61}}{k_{65}+k_{61}} \tag{A3a, b}$$

$$t_{15}=\frac{k_{12}k_{23}k_{34}k_{45}}{DEN} \qquad t_{51}=\frac{k_{54}k_{43}k_{32}k_{21}}{DEN} \tag{A4a, b}$$

or

$$t_{15}=\frac{v_{15}}{DEN} \qquad t_{51}=\frac{v_{51}}{DEN} \tag{A5}$$

with

$$DEN=k_{23}k_{34}k_{45}+k_{21}k_{34}k_{45}+k_{21}k_{32}k_{45}+k_{21}k_{32}k_{43}. \tag{A6}$$

r_1 and r_5 are the so-called reserve factors (Gradmann et al., 1981; Hansen et al.[3]). Their origin is as follows: The flux mediated by the transport system is calculated from the usual rate constants and from the law of mass action which says that the sum over all states is constant ($=N_o$). The two-state model incorporating only the interesting states N_1 and N_5 leads to an incorrect sum of states. However, all the ignored states are a linear function of N_1 and N_5, as demonstrated by Eqs. (A7) to (A12). Summing vertically over Eq. (A7) to (A12) leads to Eq. (A13). It shows that N_o can be calculated by means of the "reserve factors" r_1 and r_5.

$$N_1= \quad N_1 \tag{A7}$$

$$N_2=\frac{k_{12}}{k_{21}+\kappa_{25}}N_1+\frac{\kappa_{52}}{k_{21}+\kappa_{25}}N_5 \tag{A8}$$

$$N_3=\frac{\kappa_{13}}{\kappa_{31}+\kappa_{35}}N_1+\frac{\kappa_{53}}{\kappa_{31}+\kappa_{35}}N_5 \tag{A9}$$

$$N_4=\frac{\kappa_{14}}{\kappa_{41}+k_{45}}N_1+\frac{k_{54}}{\kappa_{41}+k_{45}}N_5 \tag{A10}$$

$$N_5= \quad 1 \quad N_5 \tag{A11}$$

$$N_6=\frac{k_{16}}{k_{61}+k_{65}}N_1+\frac{k_{56}}{k_{61}+k_{65}}N_5 \tag{A12}$$

$$N_o= \quad r_1\cdot N_1+ \quad r_5\cdot N_5. \tag{A13}$$

For the final discussion it is useful to introduce z_1 and z_5

$$r_1=1+\frac{z_1}{DEN}+\frac{k_{16}}{k_{61}+k_{65}}$$

and

$$r_5=1+\frac{z_5}{DEN}+\frac{k_{56}}{k_{61}+k_{65}}. \tag{A14a, b}$$

Replacing the gross reactions labeled "κ" by the appropriate expressions of elementary rate-constants (labeled "k") and summing vertically over Eqs. (A7) to (A12) leads to

$$z_1= \begin{array}{ccccc} 1 & 2 & 3 & 4 & 5 \\ \rightarrow & & & \rightarrow & \rightarrow \\ \rightarrow & \leftarrow & & & \rightarrow \\ \rightarrow & \leftarrow & \leftarrow & & \\ \rightarrow & \rightarrow & & & \rightarrow \\ \rightarrow & \rightarrow & \leftarrow & & \\ \rightarrow & \rightarrow & \rightarrow & & \end{array} \tag{A15}$$

$$z_5= \begin{array}{ccccc} 1 & 2 & 3 & 4 & 5 \\ & & \rightarrow & \rightarrow & \leftarrow \\ \leftarrow & & & \rightarrow & \leftarrow \\ \leftarrow & \leftarrow & & & \leftarrow \\ & & \rightarrow & \leftarrow & \leftarrow \\ \leftarrow & & & \leftarrow & \leftarrow \\ & & \leftarrow & \leftarrow & \leftarrow \end{array}. \tag{A16}$$

[2] *Ibid.*
[3] *Ibid.*

Equations (A15) and (A16) are given in a slightly unusual manner. The arrows represent rate constants labeled by the numbers at the top of the columns, e.g., the arrow at the upper left corner of Eq. (A15) signifies k_{12}. z_1 and z_5 are the sums of the products of the rate constants in each row of the scheme. This can be illustrated by rewriting Eq. (A6) as

$$DEN = \begin{array}{ccccc} 1 & 2 & 3 & 4 & 5 \\ & & \rightarrow & \rightarrow & \rightarrow \\ \leftarrow & & & \rightarrow & \rightarrow \\ \leftarrow & \leftarrow & & & \rightarrow \\ \leftarrow & \leftarrow & \leftarrow & & . \end{array} \tag{A17}$$

Introducing Eqs. (A2) and (A5) and Eqs. (A14) and (A16) into Eq. (A1) leads via

$$\phi_{in} = N_o \cdot \frac{v_{15} k_{56} k_{61}}{(k_{61}+k_{65}) DEN (r_1(t_{51}+b_{51})+r_5(t_{15}+b_{15}))} \tag{A18}$$

to

$$\phi_{in} = N_o \frac{v_{15} k_{56} k_{61}}{D} \tag{A19}$$

with

$$D = (k_{61}+k_{65})\left\{(v_{51}+v_{15})+\frac{z_1 v_{51}}{DEN}+\frac{z_5 v_{15}}{DEN}\right\} + k_{16} v_{51} + k_{56} v_{15} + z_1 k_{56} k_{61} + z_5 k_{16} k_{65} + DEN(k_{56} k_{61} + k_{16} k_{65} + k_{56} k_{16}). \tag{A20}$$

The substrate $S = [Cl]_o$ enters the equations via the bimolecular reaction

$$k_{12} = k_{12}^{00} \cdot [X]_o \cdot [Cl]_o = k_{12}^0 \cdot [Cl]_o = k_{12}^0 \cdot S. \tag{A21}$$

In Figs. 3 and 6 and Fig. 4 the influences of $[Cl]_i$ and $[H]_i$, respectively, are studied. They enter the calculation via the following equations

$$k_{65} = k_{65}^{00} \cdot [X]_i [H]_i [H]_i = k_{65}^0 [H]_i^2 = k_{65}^0 A \tag{A22}$$

and

$$k_{54} = k_{54}^{00} \cdot [XH_2^{++}]_i \cdot [Cl]_i = k_{54}^0 \cdot [Cl]_i = k_{54}^0 B. \tag{A23}$$

Extracting the dependence on S, Cl_i and H_i from z_1, z_5, v_{15} and v_{51} leads to

$$z_1 = S \cdot z_1^0 \tag{A24}$$

$$z_5 = B \cdot z_5^0 \tag{A25}$$

$$v_{15} = S \cdot v_{15}^0 \tag{A26}$$

$$v_{51} = B \cdot v_{51}^0. \tag{A27}$$

Introducing Eqs. (A22) to (A27) into Eq. (A19) leads to an equation of the Michaelis-Menten type:

$$\phi_{in} = \frac{V_{max} \cdot S}{S + K_m} \tag{A28}$$

with

$$V_{max} = \frac{v_{15}^0 k_{56} k_{61}}{(A k_{65}^0 + k_{61})\left(v_{15}^0 + z_5^0 B \frac{v_{15}^0}{DEN} + v_{51}^0 B \frac{z_1^0}{DEN}\right) + v_{15}^0 k_{56} + z_1^0 k_{56} k_{61}} \tag{A29}$$

and

$$K_m = \frac{A k_{65}^0 (DEN k_{16} + z_5^0 B k_{16} + v_{51}^0 B) + (DEN k_{56} + v_{51}^0 B)(k_{61}+k_{16})}{(A k_{65}^0 + k_{61})\left(v_{15}^0 + z_5^0 B \frac{v_{15}^0}{DEN} + v_{51}^0 B \frac{z_1^0}{DEN}\right) + v_{15}^0 k_{56} + z_1^0 k_{56} k_{61}}. \tag{A30}$$

Under the assumption that transport is energized by the membrane potential and by the pH gradient and that the pH gradient results in asymmetry of k_{23} and k_{32}, Eq. (A30) can be simplified considerably.

Introducing the conditions

$$k_{23} \gg k_{32} \quad \text{and} \quad k_{34} \gg k_{43} \tag{A31a, b}$$

results in simpler terms for

$$DEN = k_{23} k_{34} k_{45}, \quad z_1^0 = k_{12} k_{23} k_{34}, \quad z_5^0 = k_{23} k_{34} k_{54}. \tag{A32a, b, c}$$

v_{51}^0 becomes very small. These simplifications convert Eq. (A30) to

$$K_m = \frac{A^*(1-B^*) + k_{61}\left(\frac{1}{k_{16}}+\frac{1}{k_{61}}\right)}{A^*(1+B^*) + k_{61}\left(\frac{1}{k_{45}}+\frac{1}{k_{61}}+\frac{1}{k_{56}}(1+B^*)\right)} \cdot \frac{k_{16}}{k_{12}^0} \tag{A33}$$

with

$$A^* = \frac{Ak_{65}^0}{k_{56}} = \frac{k_{65}}{k_{56}} \quad \text{and} \quad B^* = \frac{k_{12}Bk_{54}^0}{k_{34}k_{45}} = \frac{k_{12}k_{54}}{k_{34}k_{45}}. \tag{A34a, b}$$

It is seen that K_m becomes independent of $A(=H_i^2)$ under the condition

$$\frac{1}{k_{16}} = \frac{1}{k_{45}} + \frac{1}{k_{56}}(1+B^*) \tag{A35}$$

i.e., K_m is independent of B^* when

$$k_{56} \gg k_{16}\, B^*. \tag{A36}$$

Eq. (A29) has the same denominator as Eq. (A30). Thus, simplifying Eq. (A29) using the assumptions of Eqs. (A31), (A32) leads to Eq. (A37), which shares the same denominator as Eq. (A33)

$$V_{max} = \frac{k_{61}}{A^*(1+B^*)+1+k_{61}\left[\frac{1}{k_{45}}+\frac{1}{k_{56}}(1+B^*)\right]}. \tag{A37}$$

Making use of Eqs. (A22) and (A23) we introduce $[Cl]_i$ and $[H]_i$:

$$A^* = \frac{k_{65}^0}{k_{56}}[H]_i^2 = A_1^*[H]_i^2 \quad \text{or}$$

$$A^* = \frac{A_1^*(\mu M)^2}{[10^{1.75}]^2}h^2 = q_h h^2 \tag{A38a, b}$$

$$B^* = \frac{k_{12}}{k_{34}}\frac{k_{54}^0}{k_{45}}[Cl]_i = q_b[Cl]_i. \tag{A39}$$

A_1^* and q_b are the values of A^* and B^* at unit concentration (1 μM in case of H_i and 1 mM in case of Cl_i). As pH = 7.75 occurs in some of the experiments discussed in this article, it leads to very handy numbers, if we make use of q_h, being the value of A_1^* at $pH_i = 7.75$ (and not at $pH_i = 6.0$, which corresponds to $[H_i] = 1$ μM). Thus $h = 10^{1.75}\ [H_i]/1\ \mu M$. Introducing Eqs. (A38) and (A39) into Eq. (A37) leads to

$$V_{max} = \frac{k_{61}/q_h}{h^2(1+q_b Cl_i)+\text{const}} \tag{A40}$$

with const being constant under conditions which lead to constant K_m (*see* Eq. A35):

$$\text{const} = \frac{1}{q_h}\left(1+k_{61}\left(\frac{1}{k_{45}}+\frac{1}{k_{56}}(1+B^*)\right)\right). \tag{A41}$$

The K_I for noncompetitive inhibition by Cl_i^- is calculated from the condition that the terms in Eq. (A40) which are Cl_i^- independent are equal to the Cl_i^- dependent terms

$$K_I = \left(\frac{\text{const}}{h^2}+1\right)\frac{1}{q_b} \tag{A42}$$

i.e., it is the concentration of Cl_i reducing V_{max} by a factor of 2.

Appendix II

Alternative Models

Inverse order of binding of H_o and Cl_o:
The gross reactions labeled by t_{15} and t_{51} have to span from the binding to the release of the transportee. In the case of reversed order of Cl_o and H_o-binding, we have to take H_o out of the *t*-rate-constants and merge it into the *b*-reactions. We do so by introducing a state 7:

$$\begin{matrix} & \rightleftharpoons 7 \rightleftharpoons 6 \rightleftharpoons 5 \\ XH_o\ X_o & \quad X_i \quad XH_i \end{matrix} \tag{A43}$$

Assuming saturating H_o concentration, we can reduce this scheme so that of Fig. 9 *A* and *B* as follows.

For this purpose the reactions $1 \rightleftharpoons 7 \rightleftharpoons 6$ are merged into the gross rate-constants

$$\kappa_{16} = \frac{k_{17}k_{76}}{k_{71}+k_{76}}; \quad \kappa_{61} = \frac{k_{67}k_{71}}{k_{71}+k_{76}}. \tag{A44a, b}$$

Saturating H_o concentration results in large k_{71}, thus

$$\kappa_{16} = \frac{k_{17}k_{76}}{k_{71}^0}\cdot\frac{1}{H_o}; \quad \kappa_{61} = k_{67} \tag{A45a, b}$$

with

$$k_{71} = k_{71}^0 \cdot H_o. \tag{A46}$$

The concentration of state 7

$$N_7 = \frac{k_{17}N_1 + k_{67}N_6}{k_{76}+k_{71}} \tag{A47}$$

can be neglected, when k_{71} becomes great. Thus r_1 and r_5 (*see* Eq. (A14)) do not need any correction in order to obey the law of conservation of mass which might be violated by introducing N_7. The above calculation shows that we can study the effect of H_o for the model in Eq. (A43) by assessing the influence of k_{61} on K_m and V_{max} in Eqs. (A30) and (A29).

References

Belkhode, M.L., Scholefield, P.G. 1969. Interactions between amino acids during transport and exchange diffusion in Novikoff and Ehrlich ascites tumor cells. *Biochim. Biophys. Acta* **173**:290

Bielby, M.J., Walker, N.A. 1980*a*. Chloride influx in *Chara:* Electrogenic and probably proton-coupled. *In:* Plant Membrane

Transport: Current Conceptual Issues. R.M. Spanswick, W.J. Lucas, and J. Dainty, editors. p. 571. Elsevier/North Holland, Amsterdam

Bielby, M.J., Walker, N.A. 1980*b*. Chloride transport in *Chara:* I. Kinetics and current voltage curves for probable proton symport. *J. Exp. Bot. (in press)*

Coster, H.G.L. 1966. Chloride in cells of *Chara australis. Aust. J. Biol. Sci.* **19**:545

Crabeel, M., Grenson, M. 1970. Regulation of histidine uptake by specific feedback inhibition of two histidine permeases. *Eur. J. Biochem.* **14**:197

Cram, W.J. 1976. Negative feedback regulation of transport in cells. The maintenance of turgor, volume and nutrient supply. *In:* Encyclopedia of Plant Physiology. Vol. 2, Part A. Transport in Cells. M.G. Pitman and U. Luttge, editors. p. 284. Springer-Verlag, Berlin

Crane, R.K. 1977. The gradient hypothesis and other models of carrier-mediated transport. *Rev. Physiol. Biochem. Pharmacol.* **78**:99

Cuppoletti, J., Segel, I.H. 1974. Transinhibition kinetics of the sulfate transport system of *Penicillium notatum:* Analysis based on an Iso Uni Uni velocity equation. *J. Membrane Biol.* **17**:239

Cuppoletti, J., Segel, I.H. 1975. Kinetics of sulfate transport by *Penicillium notatum.* Interactions of sulfate, protons and calcium. *Biochemistry* **14**:4712

Eddy, A.A. 1978. Proton-dependent solute transport in microorganisms. In: Current Topics in Membranes and Transport. F. Bronner and A. Kleinzeller, editors. Vol. 10, p. 279. Academic Press, New York

Eisenthal, R., Cornish-Bowden, A. 1974. The direct linear plot. A new graphical procedure for estimating enzyme kinetic parameters. *Biochem. J.* **139**:715

Giaquinta, R. 1980. Sucrose/proton cotransport during phloem loading and its possible control by internal sucrose concentration. *In:* Plant Membrane Transport: Current Conceptual Issues. R.M. Spanswick, W.J. Lucas, and J. Dainty, editors. p. 273. Elsevier, Amsterdam

Glass. A.D.M. 1976. Regulation of potassium absorption in barley roots: An allosteric model. *Plant Physiol.* **58**:33

Gradmann, D., Hansen, U.-P., Slayman, C.L. 1981. Reaction kinetic analysis of current-voltage relationships for electrogenic pumps in *Neurospora* and *Acetabularia. In:* Electrogenic Ion Pumps. C.L. Slayman, editor. Current Topics in Membranes and Transport, F. Bronner and A. Kleinzeller, editors. Academic Press, New York

Hansen, U.-P. 1978. Do light-induced changes in membrane potential of *Nitella* reflect the feedback regulation of a cytoplasmic parameter? *J. Membrane Biol.* **41**:197

Hansen, U.-P. 1980. Homeostasis in *Nitella:* Adaption of H^+-transport to the photosynthetic load. *In:* Plant Membrane Transport: Current Conceptual Issues. R.M. Spanswick, W.J. Lucas, and J. Dainty, editors. p. 587. Elsevier/North Holland, Amsterdam

Heinz, E., Geck, P., Wilbrandt, W. 1972. Coupling in secondary active transport. Activation of transport by co-transport and/or countertransport with the fluxes of other solutes. *Biochim. Biophys. Acta* **255**:442

Hope, A.B., Walker, N.A. 1975. The Physiology of Giant Algal Cells. Cambridge University Press, Cambridge

Hopfer, U., Groseclose, R. 1980. The mechanism of Na^+-dependent D-glucose transport. *J. Biol. Chem.* **255**:4453

Hutchings, V.M. 1978. Sucrose and proton cotransport in *Ricinus* cotyledons: I. H^+ influx associated with sucrose uptake. *Planta* **138**:229

Jensen, P., Petterson, S. 1978. Allosteric regulation of potassium uptake in plant roots. *Physiol. Plant.* **42**:207

Keifer, D.W. 1980. Alteration of cytoplasmic pH in *Chara* through membrane transport processes. *In:* Plant Membrane Transport: Current Conceptual Issues. R.M. Spanswick, W.J. Lucas, and J. Dainty, editors. p. 569. Elsevier/North Holland, Amsterdam

Komor, E., Schwab, W.G.W., Tanner, W. 1979. The effect of intracellular pH on the rate of hexose uptake in *Chlorella. Biochim. Biophys. Acta* **555**:524

Kotyk, A., Rihova, L. 1972. Transport of α-aminoisobutyric acid in *Saccharomyces cerevisiae. Biochim. Biophys. Acta* **288**:380

MacRobbie, E.A.C. 1971. Vacuolar fluxes of chloride and bromide in *Nitella translucens. J. Exp. Bot.* **22**:487

Morrison, C.E., Lichtstein, H.C. 1976. Regulation of lysine transport by feedback inhibition in *Saccharomyces cerevisiae. J. Bacteriol.* **125**:864

Pall, M.L. 1971. Amino acid transport in *Neurospora crassa.* IV. properties and regulation of a methionine transport system. *Biochim. Biophys. Acta* **233**:201

Raven, J.A. 1976. Transport in algal cells. *In:* Encyclopedia of Plant Physiology. Vol. 2, Part A. Transport in Cells. M.G. Pitman and U. Luttge, editors. p. 129. Springer-Verlag, Berlin

Raven, J.A., Smith, F.A. 1978. Effect of temperature on ion content, ion fluxes and energy metabolism in *Chara corallina. Plant Cell Environ.* **1**:231

Ring, K., Heinz, E. 1966. Active amino acid transport in *Streptomyces hydrogenans.* I. Kinetics of uptake of α-aminoisobutyric acid. *Biochem. Z.* **344**:446

Russell, J.M. 1976. ATP-dependent chloride influx into internally dialyzed squid giant axons. *J. Membrane Biol.* **28**:335

Russell, J.M. 1979. Chloride and sodium influx: A coupled uptake mechanism in squid giant axons. *J. Gen. Physiol.* **73**:801

Sanders, D. 1978. Regulation of Ion Transport in Characean Cells. Ph.D. Thesis, University of Cambridge, Cambridge

Sanders, D. 1980*a*. Control of plasma membrane Cl^- fluxes in *Chara corallina* by external Cl^- and light. *J. Exp. Bot.* **31**:105

Sanders, D. 1980*b*. Control of Cl^- influx in *Chara* by cytoplasmic Cl^- concentration. *J. Membrane Biol.* **52**:51

Sanders, D. 1980*c*. The mechanism of Cl^- transport at the plasma membrane of *Chara corallina:* I. Cotransport with H^+. *J. Membrane Biol.* **53**:129

Segel, I.H. 1975. Enzyme Kinetics. Wiley & Sons, New York

Smith, F.A., Walker, N.A. 1976. Chloride transport in *Chara corallina* and the electrochemical potential for hydrogen ions. *J. Exp. Bot.* **27**:451

Tazawa, M., Kikuyama, M., Shimmen, T. 1976. Electric characteristics and cytoplasmic streaming of characeae cells lacking tonoplast. *Cell. Struct. Funct.* **1**:165

Williamson, R.E. 1975. Cytoplasmic streaming in *Chara:* A cell model activated by ATP and inhibited by cytochalasin B. *J. Cell Sci.* **17**:655

Received 16 June 1980; revised 23 September 1980